ELSEVIER

Brain Research 645 (1994) 201–214

BRAIN RESEARCH

Research Report

# A neuronal network from the mollusc *Lymnaea stagnalis*

Neil S. Magoski *, Naweed I. Syed, Andrew G.M. Bulloch

*Departments of Anatomy and Medical Physiology, and Neuroscience Research Group, Faculty of Medicine, University of Calgary, 3330 Hospital Drive NW, Calgary, Alta., T2N 4N1, Canada*

(Accepted 25 January 1994)

**Abstract**

The morphology, electrophysiology, and synaptic inputs of a ventrally located neuronal network from the CNS of the pond snail *Lymnaea stagnalis* was investigated. Three large, previously identified neurons [55] known as right parietal ventral one, two, and three (RPV1,2,&3) were found to be electrically coupled to one another. Coupling between either RPV1&2 or RPV1&3 was weak while coupling between RPV2&3 was strong. Consistent bursting activity was observed in neuron RPV1 while neurons RPV2&3 were either silent or fired tonically. When isolated in vitro, similar patterns of activity could be elicited in neurons RPV1–3. Lucifer yellow staining revealed that these cells send axons through nerves innervating musculature involved in locomotion, whole-body withdrawal, and cardio-respiratory function. Neurons RPV1–3 were found to be inhibited by an identified interneuron, visceral dorsal four, known to be directly involved in cardio-respiratory behavior [43]. Furthermore, neurons RPV1-3 were also inhibited by a wide-acting synaptic input, known as Input three [9], which is associated with respiratory pattern generation [43]. An interneuron, identified as right pedal dorsal eleven (RPeD11), which coordinates locomotory and withdrawal behavior [44], was found to excite neuron RPV1. When neurons RPeD11 and RPV1 were isolated in vitro and allowed to extend neurites, they formed a synaptic connection similar to that observed in the isolated brain. In vitro work on these neurons may make them an attractive model to study synapse formation and bursting activity.

*Key words:* Chemical synapse; Electrical synapse; Conditional bursting; Cell culture; Synapse formation; Circuit

## 1. Introduction

One of the major goals of neurobiology is to understand the neural circuitry responsible for brain function. The large, identified neurons of some invertebrates have provided opportunities to analyze the circuits underlying specific behaviors in great detail [20, 24,26,32,40]. The gastropod nervous system, with its small numbers of neurons and large identifiable neuronal somata, is advantageous for studying neural circuits [3,7,20,24,28,32,40].

One gastropod used extensively in neuroethology is the freshwater pond snail, *Lymnaea stagnalis*. Using this animal, many networks have been identified [6,16, 32,40,43,47,49]. It is worth noting that the mapping of networks in *Lymnaea* has been confined primarily to the dorsal surface of the CNS, while little is known about ventral neurons – especially in the central ring ganglia [29,36]. Consequently, it is important to describe the morphology, electrophysiology, and connectivity of neurons located on the ventral surface of *Lymnaea's* CNS, in particular, neurons that are readily identified. Furthermore, the relationship of these neurons to known neural networks is also significant for the use of *Lymnaea* as a neurobiological model.

Beyond the characterization of neural circuits, research on gastropod neurons has been approached using identified cell culture [13,38,60] and *Lymnaea* is no exception [45,46]. This technique has lead to the reconstruction and analysis of specific, and behaviorally relevant, neural circuits [33,45]. Furthermore, the isolation and culture of molluscan cells provides information on the intrinsic properties of the individual neurons themselves [15,52,53] as well as the formation and functioning of their synaptic interactions [21,46].

In the present study, a network of electrically and chemically connected neurons is examined at both the

* Corresponding author. Department of Medical Physiology, Faculty of Medicine, University of Calgary, 3330 Hospital Drive NW, Calgary, Alberta, Canada T2N 4N1. Fax: (1) (403) 283-8731.


*SSDI* 0006-8993(94)00154-5

in situ and in vitro levels. Both the intrinsic and network properties of a group of previously identified neurons [55] known as *right parietal ventral 1–3 (RPV1-3)* are characterized. Furthermore, the interactions between locomotory and respiratory interneurons and neurons RPV1-3 is also investigated. The in vitro investigation of this network may contribute to our understanding of intrinsic neuronal firing and specific synapse formation.

## 2. Materials and methods

### 2.1. Animals

This study employed a laboratory stock of the pulmonate mollusc, *Lymnaea stagnalis*, established from the Free University of Amsterdam. Animals used for histology, electrophysiology, and preparation of conditioned medium had shell lengths of 20–25 mm (age ~2–4 months) whereas animals used in cell culture were 15–20 mm (age ~1–2 months) in length.

### 2.2. Dissection and salines

The central nervous system (CNS) was removed and pinned out flat, either dorsal or ventral side up, to the silicone rubber (RTV #616 GE) base of a 60 mm Petri dish. Dissections and most electrophysiology were performed in normal *Lymnaea* saline (composition in mM: NaCl 51.3, KCl 1.7, $CaCl_2$ 4.1, $MgCl_2$ 1.5, and *N*-2-hydroxyethylpiperazine-*N'*-2-ethanesulphonic acid (HEPES) 5.0; pH 7.9). To test for chemical synapses, a low $Ca^{2+}$/high $Mg^{2+}$ saline was used (composition in mM: NaCl 51.3, KCl 1.7, $CaCl_2$ 0, $MgCl_2$ 1.5, $MgSO_4$ 13.5 mM, and HEPES 5.0; pH 7.9). To test for monosynaptic chemical transmission, a high $Ca^{2+}$/high $Mg^{2+}$ saline was employed (composition in mM: NaCl 51.7, KCl 1.7, $CaCl_2$ 24.6, $MgCl_2$ 1.5, $MgSO_4$ 7.5, and HEPES 5.0; pH 7.9). Work was performed at a room temperature of 18–20°C.

### 2.3. Electrophysiology

Electrophysiology was undertaken on in situ brain preparations and cultured neurons. Intracellular recordings were made using single-barrel micropipettes pulled from 1.5 mm diameter, filamented borosilicate glass – when filled with 0.75 M KCl these electrodes had a final resistance of 30–40 MΩ. Electrophysiological data were collected using either a Neurodata dual channel intracellular amplifier (IR #283) or Dagan cell explorer amplifiers (#8100). Microelectrodes were connected to the amplifier headstage via a silver wire coated with AgCl. The voltage signal was displayed on Tektronix dual beam and Nicolet digital storage oscilloscopes, and recorded on a Gould 2 channel or 6 channel chart recorder. Microelectrodes were bridge balanced with 20 ms, 1 nA square, hyperpolarizing current pulses. Current was injected into the neurons using either the direct current injection function on the amplifier or the stimulator itself. A silver wire coated with AgCl served as ground. To facilitate microelectrode penetration, the sheath surrounding the CNS was exposed to a small pronase crystal (Sigma, type XIV); following a rinse in cold (~4°C) normal saline, the inner sheath was carefully removed with fine forceps to expose the neurons.

### 2.4. Lucifer yellow staining

The morphology of identified neurons was examined by staining with Lucifer yellow. Microelectrode tips were filled with a 4% w/v solution of Lucifer yellow CH, lithium salt (Molecular probes, L-453) dissolved in 0.1% LiCl, the shaft of the microelectrode was then filled with 0.1% LiCl. Following impalement, the dye was injected with constant 0.5–1.0 nA hyperpolarizing current for 5–30 min. A neuron was considered stained when the soma fluoresced brightly under a blue filter (Schott, BG-12) mounted on a tungsten light source. Once stained, the preparations were left overnight at 4°C in normal saline and then fixed for 3 h in 3.7% formaldehyde v/v in phosphate buffer (132.3 mM $Na_2HPO_4$ and 25.2 mM $NaH_2PO_4 \cdot H_2O$, pH 7.3). Preparations were then dehydrated in a series of ethanol washes: 50%, 70%, 90%, and 100% ethanol (2×30 min). Subsequently, the preparations were defatted for 10 min in dimethyl sulfoxide, then cleared and mounted in methyl salicylate on glass slides. Stained neurons were viewed on a Zeiss Universal microscope using epifluorescence. A band pass excitation filter (BP 436/8 nm), both long and short pass barrier filters (LP 500 nm & KP 600 nm), and a 510 nm dichroic mirror were employed. Photographs were taken using negative film.

### 2.5. Identified cell culture

Identified cell culture was performed according to similar procedures described by Ridgway et al. [35]. Prior to dissection, the de-shelled snails were soaked (5 min) in 25% Listerine in normal saline. Animals were then placed in antibiotic saline (ABS; normal saline with 150 μg/mL of gentamycin; Sigma, #G3632) and the brains removed under aseptic conditions. Following a 15-min wash in ABS, the brains were placed in an enzyme cocktail of 1.33 mg/ml collagenase/dispase (Boehringer Mannheim, #269638) and 0.67 mg/ml trypsin (Sigma, type III) in defined medium (DM) for 30–40 min. The DM used was serum-free 50% Liebowitz L-15 medium (GIBCO, special order) with added inorganic salts (concentration in mM: NaCl 40.0, KCl 1.7, $CaCl_2$ 4.1, $MgCl_2$ 1.5, and HEPES 10.0; pH 7.9) and 20 μg/mL of gentamycin. After enzyme treatment, the brains were placed for 10 min in a 0.67 mg/ml solution of soybean trypsin inhibitor (Sigma, type I-S) dissolved in DM. The brains were then pinned to the rubber (RTV 616 GE) base of a 60 mm petri dish containing high osmolarity DM (DM containing an additional 30 mM glucose). The inner sheath was removed from the ganglia of interest and identified neurons were isolated by employing a siliconized, fire-polished pipette attached to a micrometer syringe for vacuum or pressure. Isolated cells were placed on poly-L-lysine coated (Sigma, P-6516) 35 mm petri dished (Falcon #3001) – coating procedure according to Wong et al. [59]. The dishes contained 1 ml DM mixed with 1 ml of conditioned medium (CM). The CM was made by incubating DM with the CNS from other *Lymnaea* at 2 brain/ml for 72 h; subsequently, the CM was filtered through a 0.22 μm filter (low protein binding, Millipore, #SL0V025LS) and frozen in 10 ml tubes (Falcon, #2006) at −70°C. The conditioned medium was thawed and gently agitated just before use – it is required to promote neurite outgrowth from cultured cells [59,60]. Cultured neurons were viewed on a Zeiss inverted microscope and photographed using negative film.

### 2.6. Statistical analysis

To test for a significant difference between two means, the two-tailed Student's *t*-test of independent means was used [31]. The criterion for significance or '*P*-value' was 0.05. The mean and standard error of the mean are reported throughout.

## 3. Results

This work describes a group of electrically connected neurons that receive chemical synaptic inputs

from several identified interneurons. The morphology of these coupled cells and the nature of the inputs they receive are illustrated. Furthermore, the in vitro properties of the individual neurons and the re-establishment of one of their inputs is demonstrated.

### 3.1. Identified neurons

This study encompasses several previously identified neurons and neuronal clusters. Fig. 1A shows a schematic diagram of *Lymnaea's* central ganglionic ring. Labelled are the interneuron right pedal dorsal eleven (RPeD11) [44], the cardio-respiratory interneuron visceral dorsal four (VD4) [11,43], and the cardio-respiratory cell cluster of visceral H,I,J,K cells [9,11, 43,47]. In Fig. 1B, a ventral view of the four lower central ring ganglia is displayed. Illustrated are three large neurons known as right parietal ventral one–three (RPV1–3) [55].

### 3.2. Morphology of neurons RPV1–3

Neurons RPV1–3 are the largest cells on the ventral surface of the right parietal ganglion and have a medial, slightly anterior location. Although these cells have been previously identified [50,55], their morphology was not studied and their electrophysiological description was brief. Neuron RPV1 is the largest and whitest of the three (soma diameter of 120–170 $\mu$m); whereas neurons RPV2&3 are somewhat smaller

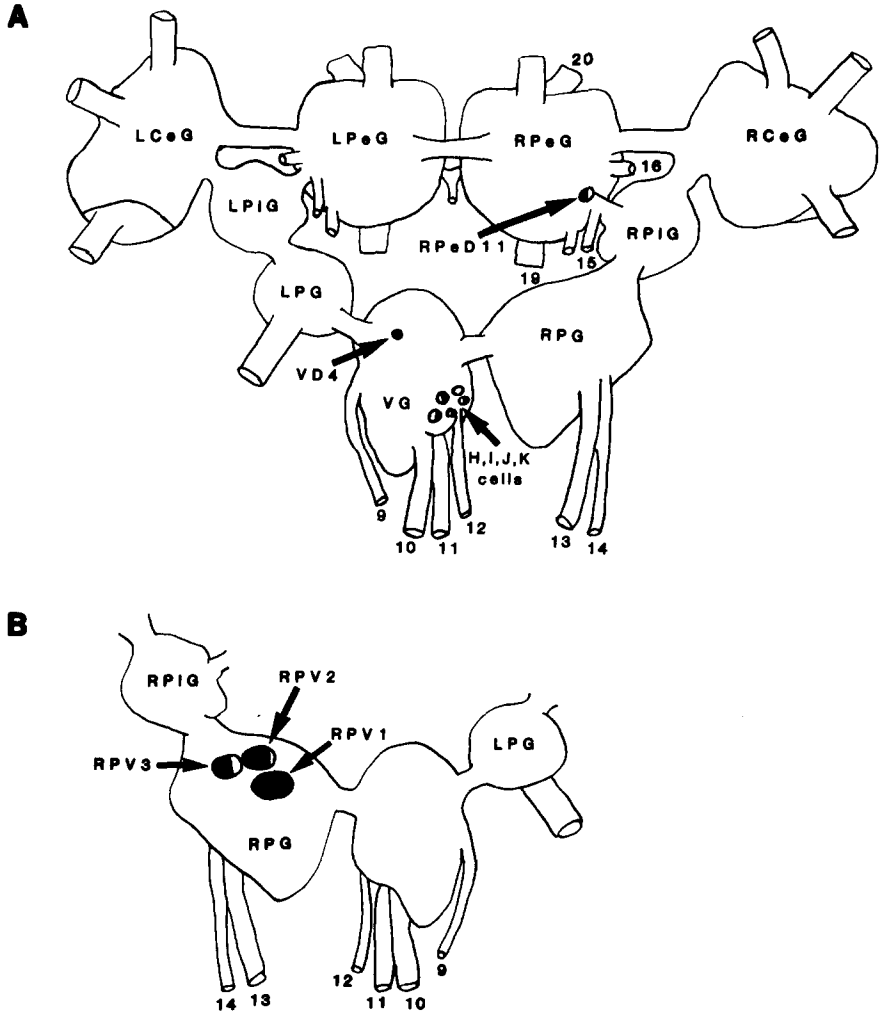


Fig. 1. Schematic maps of the *Lymnaea* CNS. A: *Lymnaea's* central ring ganglia; abbreviations for the ganglia are as follows: left and right cerebral ganglia (LCeG & RCeG), left and right pedal ganglia (LPeG & RPeG), left and right pleural ganglia (LPlG & RPlG), left and right parietal ganglia (LPG & RPG), and the visceral ganglion (VG). Indicated are the locations of neuron right pedal dorsal eleven (RPeD11), neuron visceral dorsal four (VD4), and a cluster of neurons known as the visceral H,I,J,K cells. B: ventral surface of the lower four ganglia from the central ring. The arrows indicate neurons right parietal ventral one, two, and three (RPV1,2,&3). Shading denotes white coloration in the cells while no shading indicates orange coloration. The relevant visceral, parietal, and pedal nerves are numbered according to the convention of Slade et al. [41]: cutaneous pallial (9), intestinal (10), anal (11), genital (12), right internal parietal (13), right external parietal (14), right inferior cervical (15), right superior cervical (16), right inferior pedal (19), right medial pedal (20).

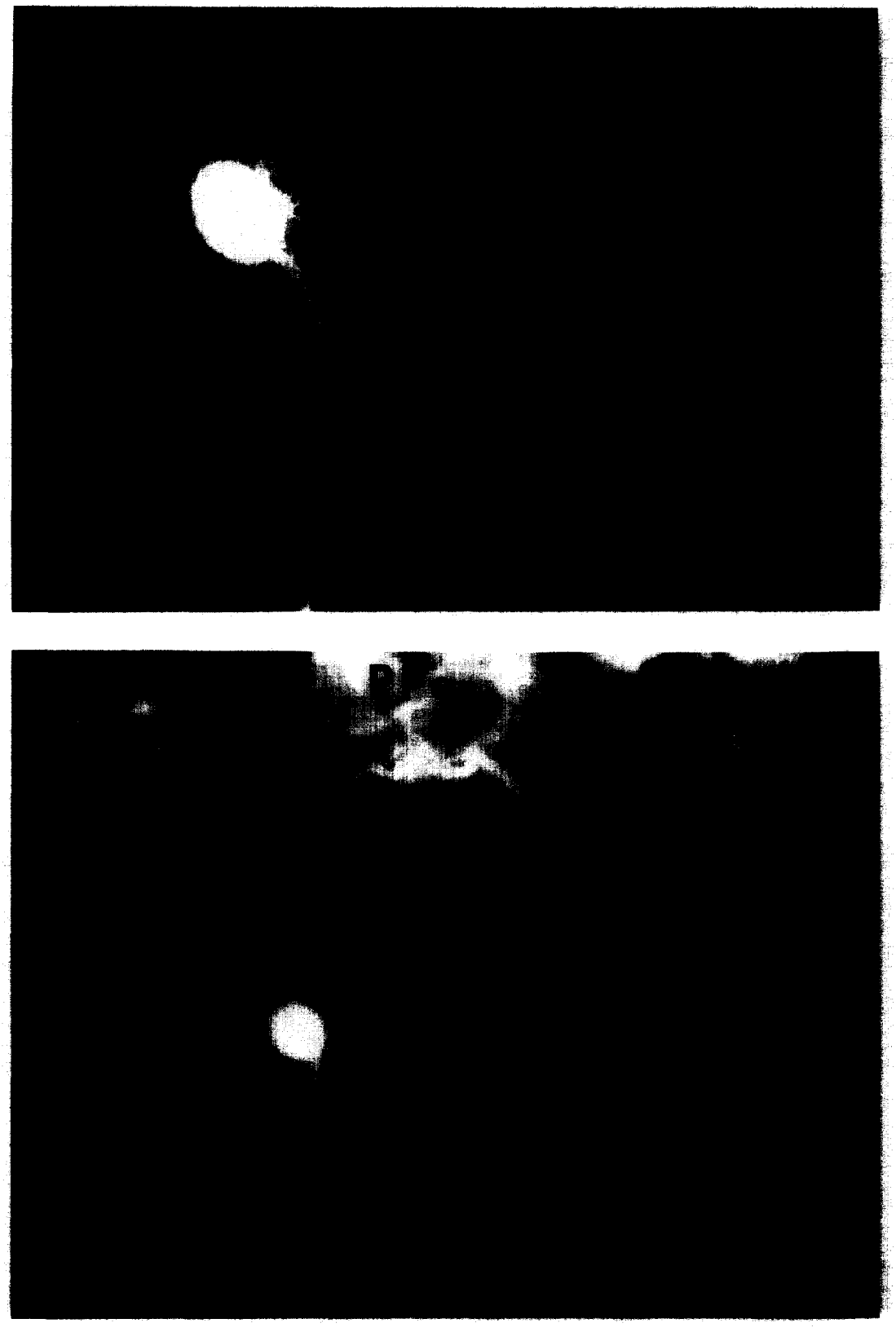

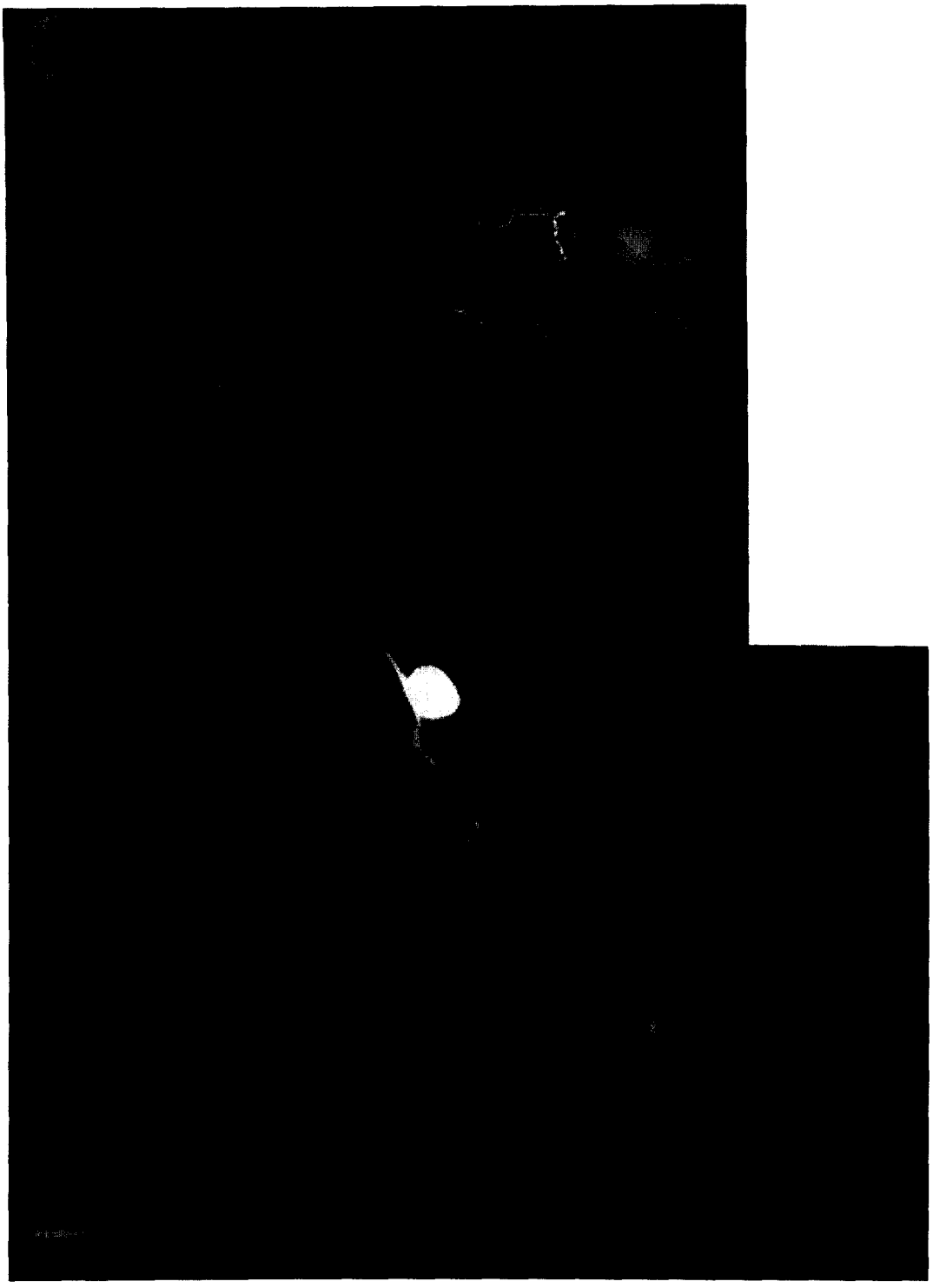

Fig. 2. Morphology of neurons RPV1–3 as revealed by Lucifer yellow staining. A: neuron RPV1 has an arbor of neurites confined to the right parietal ganglion and a single axon which projects through the right internal parietal nerve (13). B: staining of neuron RPV2 shows a lattice-like arbor in the right parietal and right pleural ganglia. This cell sends axons projecting through the right internal parietal nerve (13), genital nerve (12), intestinal nerve (10), cutaneous pallial nerve (9), right inferior cervical nerve (15), and the inferior pedal nerve (19). C: Neuron RPV3 sends axons through the right internal parietal nerve (13), anal nerve (11), right inferior cervical nerve (15), right superior cervical nerve (16), and right medial pedal nerve (20). Nerves are numbered according to the convention of Slade et al. [41]. The abbreviations for the ganglia are as follows: right parietal ganglion (RP), visceral ganglion (V), right cerebral ganglion (RCe), right pedal ganglion (RPe), and right pleural ganglion (RPl). All scale bars are 100 $\mu$m.

Table 1
Morphology of neurons RPV1–3

| Neuron | Nerve | | | | | | | | | |
|---|---|---|---|---|---|---|---|---|---|---|
| | CP (9) * | I (10) | A (11) | G (12) | RIP (13) | REP (14) | RIC (15) | RSC (16) | RIPe (19) | RMPe (20) |
| RPV1 | – | – | – | – | + | – | – | – | – | – |
| RPV2 | + | + | V | + | + | V | + | V | + | + |
| RPV3 | – | – | + | – | + | V | + | + | – | + |

* Nerve number according to the nomenclature of Slade et al. [41] (see also Fig. 1).
The (+) sign indicates that an axon was always found in the nerve, a (–) sign indicates that an axon was never found in the nerve, and a (V) indicates that a variable number of preparations had axons in the nerve. The nerves abbreviations are as follows: cutaneous pallial (CP), intestinal (I), anal (A), genital (G), right internal parietal (RIP), right external parietal (REP), right inferior cervical (RIC), right superior cervical (RSC), right inferior pedal (RIPe), right medial pedal (RMPe).

(somata diameters of 100–120 $\mu$m) and slightly orange in color. From both the position of the neuronal somata and the extent of the axonal arbors (see description below), it is reasonable to propose that neurons RPV1–3 are in physical contact.

Lucifer yellow staining of neuron RPV1 ($n = 30$) revealed a single axon projecting through the right internal parietal nerve (RIPN) (Fig. 2A, Table 1). This cell also exhibited a small arbor of axon collaterals that remained within the confines of the ganglion. An attempt was made to trace neuron RPV1's axon to its peripheral target(s) through the RIPN – a nerve which innervates the pneumostome or breathing orifice of *Lymnaea* [41]. The axon of neuron RPV1 was traced through the RIPN to the anterior pneumostome area and then seen to dive deeper into the body wall ($n = 10$; data not shown).

Staining of neuron RPV2 showed an extensive axonal branching pattern and a lattice-like arbor in the right parietal and right pleural ganglia (Fig. 2B, Table 1). In most preparations ($n = 15$), axons from neuron RPV2 projected through the right internal parietal nerve, genital nerve, intestinal nerve, cutaneous pallial nerve, right inferior cervical nerve, and the right inferior pedal nerve. Neuron RPV2 also sends an axon through the medial pedal nerve (not visible in Fig. 2B) and projections that appear to terminate in the right cerebral ganglion. There were some variations in this projection pattern ($n = 5$ additional), including additional projections through the anal nerve, right external parietal nerve, or the right superior cervical nerve.

The morphology of neuron RPV3 was similar to that of neuron RPV2; however, its axonal projections were somewhat less diverse (see Fig. 2C, Table 1). This

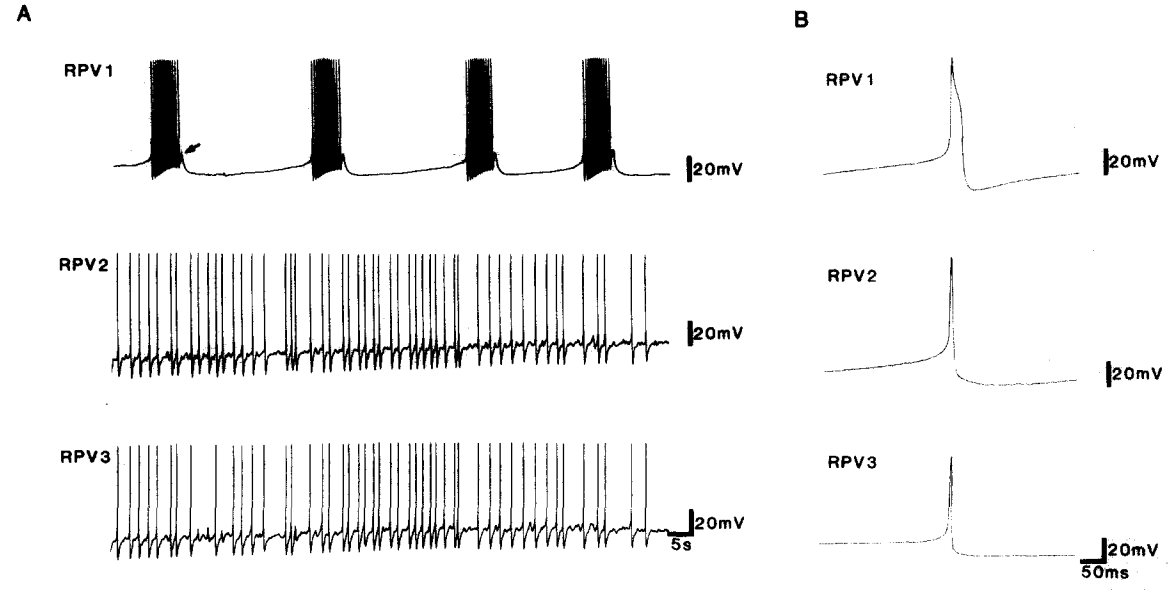


Fig. 3. Electrophysiology of neurons RPV1–3 in the isolated brain. A: the most frequently observed firing patterns of neurons RPV1–3. Distinct bursting is seen in neuron RPV1 while neurons RPV2&3 show tonic firing. Note the characteristic shape of the burst in neuron RPV1 especially the depolarizing afterpotential (indicated with the arrow after the first burst). B: action potential wave forms of neurons RPV1–3. Neuron RPV1's action potential possessed a distinct shoulder on the falling phase and was always longer in duration than those observed in neurons RPV2&3.

neuron ($n = 17$) was found to have axons projecting through the right internal parietal nerve, anal nerve, right superior cervical nerve, right inferior cervical nerve, right medial pedal nerve. Like neuron RPV2, neuron RPV3 had projections that terminated in the right cerebral ganglia. The variation in this projection pattern was slight, consisting of an extra axon in the right external parietal nerve ($n = 6$ additional). See Table 1 for a summary of the branch patterns of neurons RPV1-3 and their variability.

### 3.3. Electrophysiology of neurons RPV1–3

The basic electrophysiological properties, i.e., firing pattern, action potential half-width, and input resistance, of neurons RPV1–3 were determined using isolated brain preparations. Neuron RPV1 was found to have a characteristic, but variable, bursting pattern of activity ($n = 68$). The bursts were usually 5–15 s in length, composed of 10–25 attenuating action potentials, and separated by an interburst interval of 10–20 s (Fig. 3A). Immediately following the last action potential of each burst, neuron RPV1 displayed a characteristic depolarizing afterpotential – a phenomenon associated with burst termination in some neurons [1]. Although bursting was the usual firing pattern observed in neuron RPV1, occasionally it was silent or fired tonically at less than 1 Hz. Conversely, neurons RPV2&3 ($n = 15$ and 17) did not exhibit true bursting but showed either tonic firing at 0.5–2 Hz (Fig. 3A) or periods of quiescence. When not firing, neurons RPV1–3 had membrane potentials of −55 to −60 mV.

A distinguishing feature of neurons RPV1–3 was the duration of their action potential. Action potential duration and shape has been used in the past to distinguish between *Lymnaea* neurons [9,54,57]. The action potential half-width was measured by first determining a point on the voltage sweep, 20 ms prior to the peak of the action potential. The voltage difference between this point and the peak of the action potential was halved and designated as the half-way point along the rising phase. The half-width was then determined by measuring the distance (time in ms) from the rising phase half-way point to a corresponding, parallel point on the falling phase of the action potential. The action

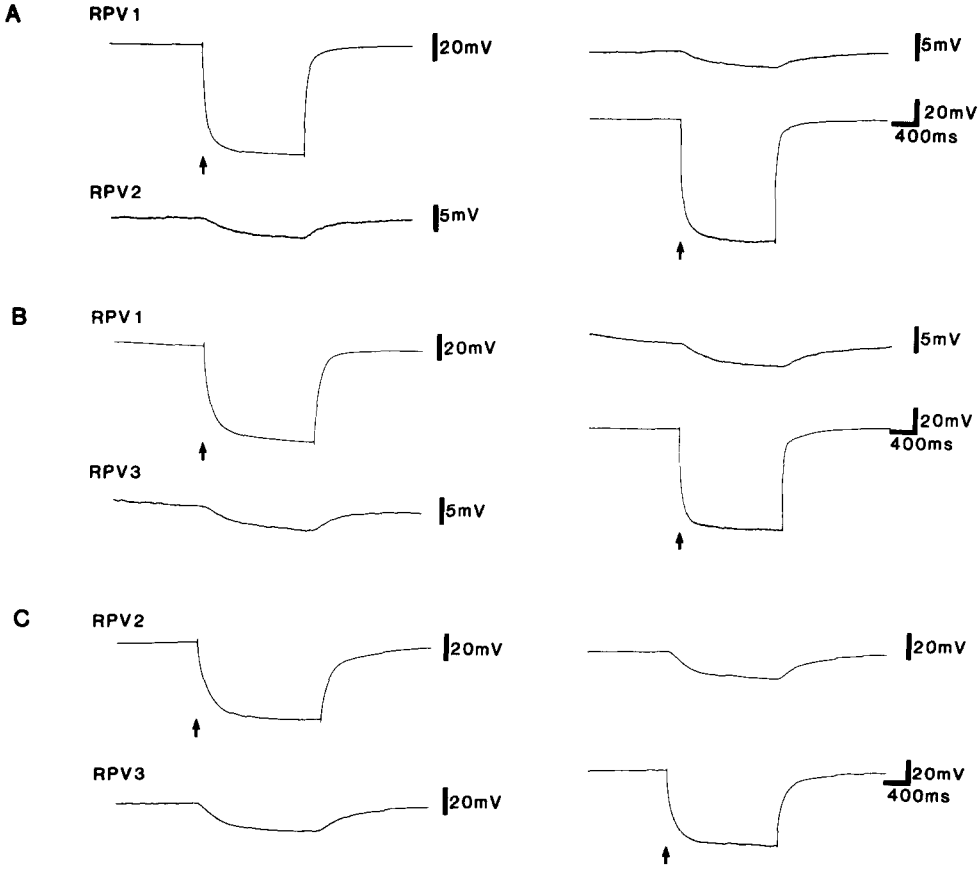


Fig. 4. Electrical coupling between neurons RPV1–3. Arrows indicate when, and to what neuron, hyperpolarizing current was delivered. A,B: coupling was weak, in both directions, between neurons RPV1&2 or neurons RPV1&3. C: coupling was strong between neurons RPV2&3.

Table 2
Action potential half-width and input resistance of neurons RPV1–3 in the isolated brain

| Neuron | Action potential half-width (ms) * | n | Input resistance (MΩ) † | n |
|---|---|---|---|---|
| RPV1 | 18.8 ±2.2 | 10 | 56.5±3.6 | 13 |
| RPV2 | 5.25±0.6 | 10 | 45.7±5.7 | 14 |
| RPV3 | 3.6 ±0.3 | 10 | 46.8±2.9 | 10 |

* The action potential half-width of neuron RPV1 was statistically different from those of neurons RPV2&3; furthermore, neurons RPV2&3 also had statistically different half-widths.
† No statistical difference was detected between the input resistance values.

potential of neuron RPV1 possessed a shoulder and was consistently broader than those of RPV2 or 3 (Table 2).

The input resistance of neurons RPV1–3 was similar (Table 2). Resistance was calculated by using Ohm's law ($V = I/R$). Voltage was measured by passing 2 s, 1.0 nA, square hyperpolarizing current pulses into a neuron and measuring the steady-state voltage drop.

### 3.4. Electrical coupling between neurons RPV1–3

Electrical coupling was observed between neurons RPV1–3 in the isolated brain preparation. Coupling was measured with 1 electrode in each cell and by passing a ~2 s, 1.0–2.0 nA, square current pulse into one of the neurons; subsequently, the voltage drops from the two cells were determined and the coupling coefficient ($V_2/V_1$) calculated. Coupling between neurons RPV1&2 or RPV1&3 was weak, with coupling coefficients of approximately 0.05 in both cases (Figs. 4A,B). However, coupling between neurons RPV2&3 was much stronger, with a coupling coefficient of approximately 0.3 (Fig. 4C; Table 3).

### 3.5. Properties of neurons RPV1–3 in vitro

The firing patterns displayed by neurons RPV1–3 suggested that these cells may have endogenous bursting properties. To test this, the electrophysiological behavior of neurons RPV1–3 was examined in vitro.

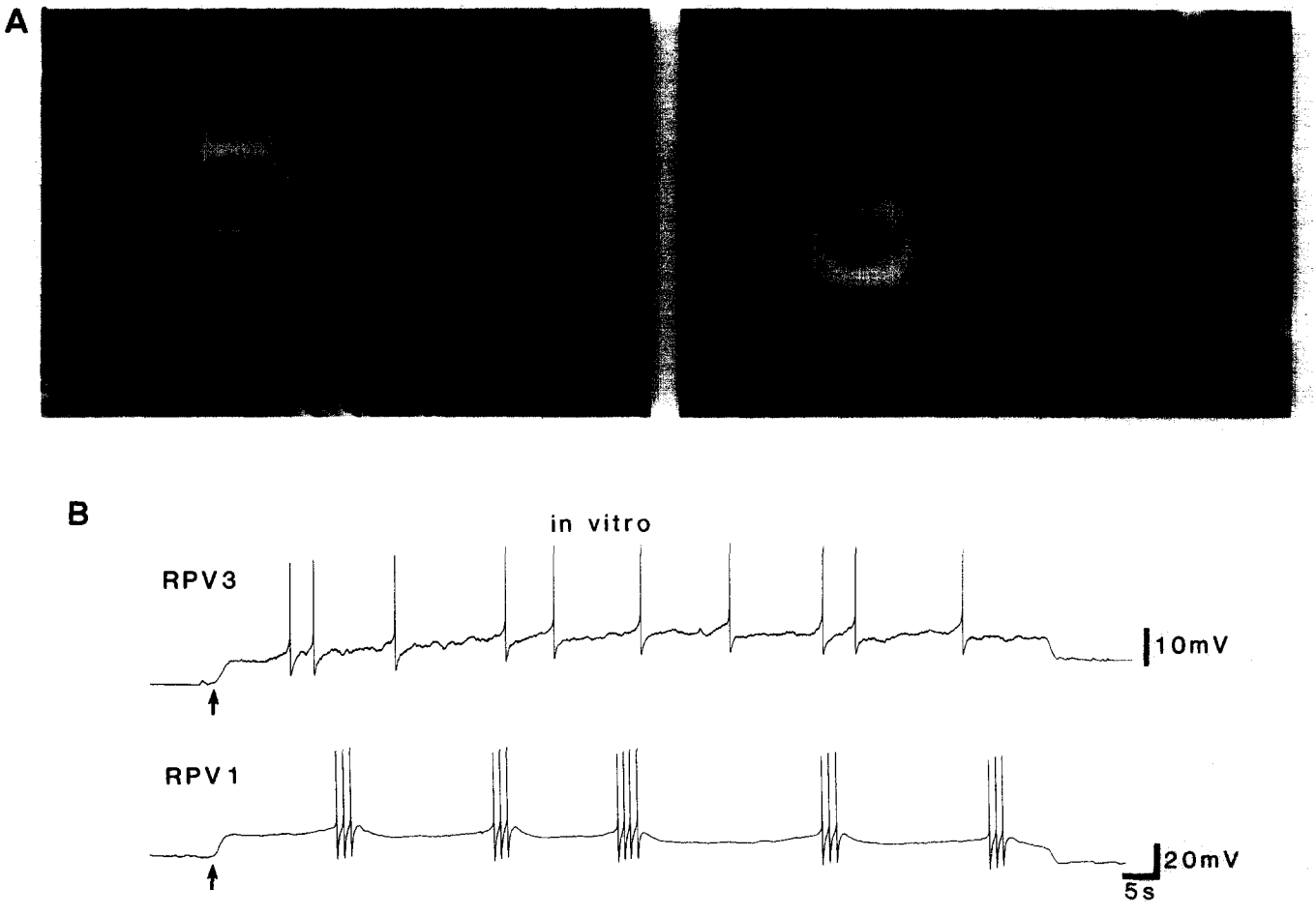


Fig. 5. Morphology and electrophysiology of neurons RPV1&3 in vitro. A: neurons RPV1 (right) and RPV3 (left) plated in CM for 1 day. These cells are in the same dish but do not have physical contact. Scale bar is 100 μm. B: electrophysiology of the cells shown in part A. Upon the injection of constant depolarizing current (at arrows), neuron RPV1 fired bursts and neuron RPV3 fired single spikes. Note the distinct depolarizing afterpotentials at the end of neuron RPV1's burst.

Table 3
Electrical coupling between neurons RPV1–3

| Coupling relationship * | Coupling coefficient | n |
|---|---|---|
| RPV1 to RPV2 | 0.051 ± 0.010 | 8 |
| RPV2 to RPV1 | 0.047 ± 0.005 | 9 |
| RPV1 to RPV3 | 0.054 ± 0.005 | 8 |
| RPV3 to RPV1 | 0.048 ± 0.006 | 9 |
| RPV2 to RPV3 | 0.344 ± 0.032 | 11 |
| RPV3 to RPV2 | 0.305 ± 0.031 | 13 |

* The coupling relationship denotes the direction in which the current was injected into the cells. For example, 'RPV1 to RPV2' indicates that current was injected into neuron RPV1 and transferred to neuron RPV2.

Neurons RPV1–3 were removed from the ganglion and plated on poly-L-lysine coated dishes in the presence of conditioned medium (CM). Under those conditions the cells exhibited neurite outgrowth (Fig. 5A). Electrophysiological investigation of these cells revealed some differences from the in vivo situation. The resting membrane potentials of these neurons was −45 to −60 mV, which is similar, although broader, than the range observed in the isolated brain. Following impalement, the cultured cells fired a few action potentials and then became quiescent – the neurons did not burst or fire tonically. However, when cells were injected with a small amount of depolarizing current, they fired patterns of action potentials qualitatively similar to that observed in the isolated brain, i.e., neuron RPV1 fired distinct bursts with depolarizing afterpotentials and neurons RPV2&3 fired single, random action potentials ($n = 6,4,\&5$ for neurons RPV1,2,&3 respectively) (Fig. 5B).

### 3.6. Synaptic inhibition of neurons RPV1–3 by cardio-respiratory interneurons in situ

Neurons RPV1–3 received inhibitory synaptic inputs from two interneurons known to be involved in cardio-respiratory behavior. The first of these inputs was an inhibitory chemical synapse from the identified interneuron visceral dorsal four (VD4; see Fig. 1A) [11,43]. In order for recordings to be made from both dorsal and ventral cells, the right parietal ganglion was twisted to expose its ventral surface. When neuron VD4 was stimulated, it inhibited either burst or tonic activity in neurons RPV1–3 ($n = 7$) (Fig. 6). This connection was maintained in a high $Ca^{2+}$/high $Mg^{2+}$ saline ($n = 3$), suggesting monosynaptic transmission (Fig. 6). The high $Ca^{2+}$/high $Mg^{2+}$ saline is considered an effective test of monosynaptic transmission because it raises the threshold of firing of any unknown, intercalated neurons between the cells in question [4,10,17].

The second source of inhibition came from a wide-acting synaptic input known as Input 3 (Ip.3) [9]. The

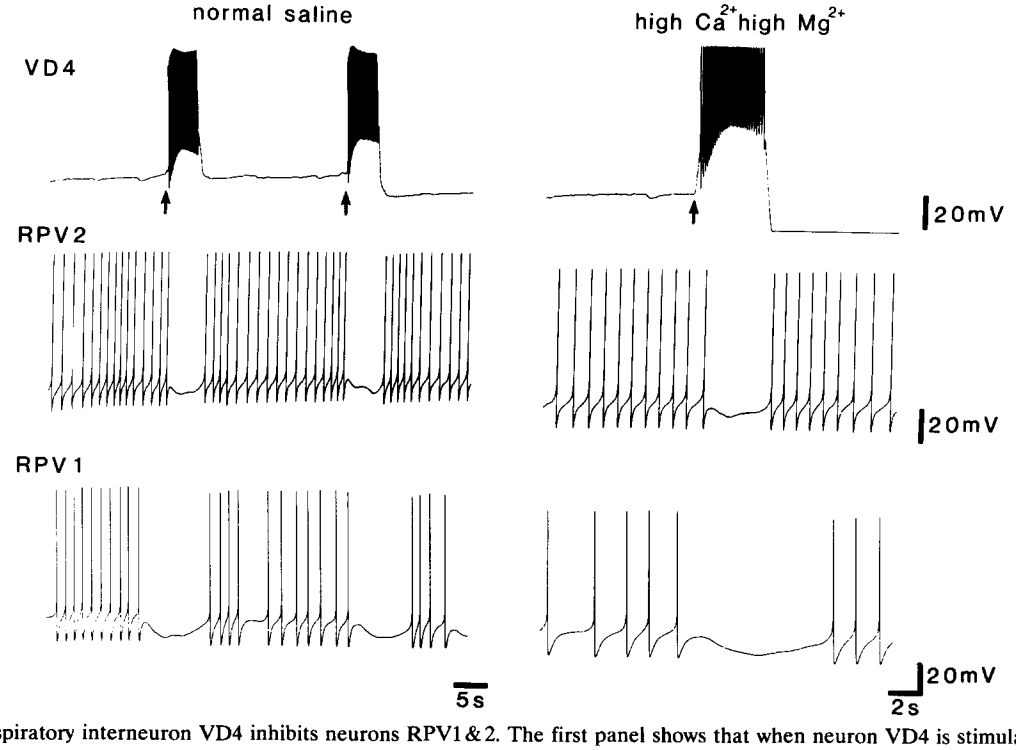


Fig. 6. Cardio-respiratory interneuron VD4 inhibits neurons RPV1&2. The first panel shows that when neuron VD4 is stimulated (at arrows) it inhibits firing in neurons RPV1&2. It appears that neuron VD4 inhibits neuron RPV1 by inducing burst termination, i.e., depolarizing afterpotentials are present. The second panel shows that this inhibitory chemical synapse persists in a high $Ca^{2+}$/high $Mg^{2+}$ saline – suggesting monosynaptic transmission.

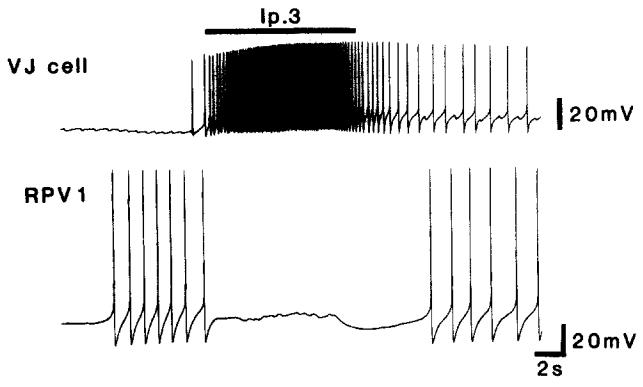


Fig. 7. The wide-acting synaptic input known as input three (Ip.3) inhibits neuron RPV1. Ip.3 produces a unique firing pattern in a visceral J (VJ) cell – as indicated by the bar. During Ip.3 activity, neuron RPV1 undergoes burst interruption, made conspicuous by the absence of a depolarizing afterpotential. Following inhibition, neuron RPV1 begins to fire again.

activity of Ip.3 can be monitored through its characteristic effect on its follower cells [9]; for example, Ip.3 produces a dramatic burst of action potentials in the Visceral J cells (VJ cells; see Fig. 1A) – a group of follower cells which are respiratory motor neurons [43]. When such activity was observed in a VJ cell, there was a corresponding inhibition of burst activity in neurons RPV1–3 ($n = 7$) (Fig. 7). During such inhibition, neuron RPV1 displayed early and uncharacteristic burst termination, i.e., there was no depolarizing afterpotential during the Ip.3 discharge; rather, the action potentials would simply cease (see Fig. 7).

### *3.7. Synaptic excitation of neuron RPV1 by interneuron RPeD11 in situ and in vitro*

An identified interneuron, known as right pedal dorsal eleven (RPeD11; see Fig. 1A) [44] excited neuron RPV1 in the isolated brain preparation ($n = 10$). Again, the right parietal ganglion was twisted so that its ventral surface was exposed and both dorsal and ventral cells could be investigated simultaneously. Stimulation of neuron RPeD11 increased the firing frequency of neuron RPV1 during a burst (Fig. 8A), i.e., the burst phase of neuron RPV1 could be altered by neuron RPeD11. This connection was demonstrated to be chemical and probably monosynaptic because it was abolished in low $Ca^{2+}$/high $Mg^{2+}$ saline and it persisted in high $Ca^{2+}$/high $Mg^{2+}$ saline ($n = 13$) (Fig. 8B). On several occasions (7 out of 13), the EPSP had

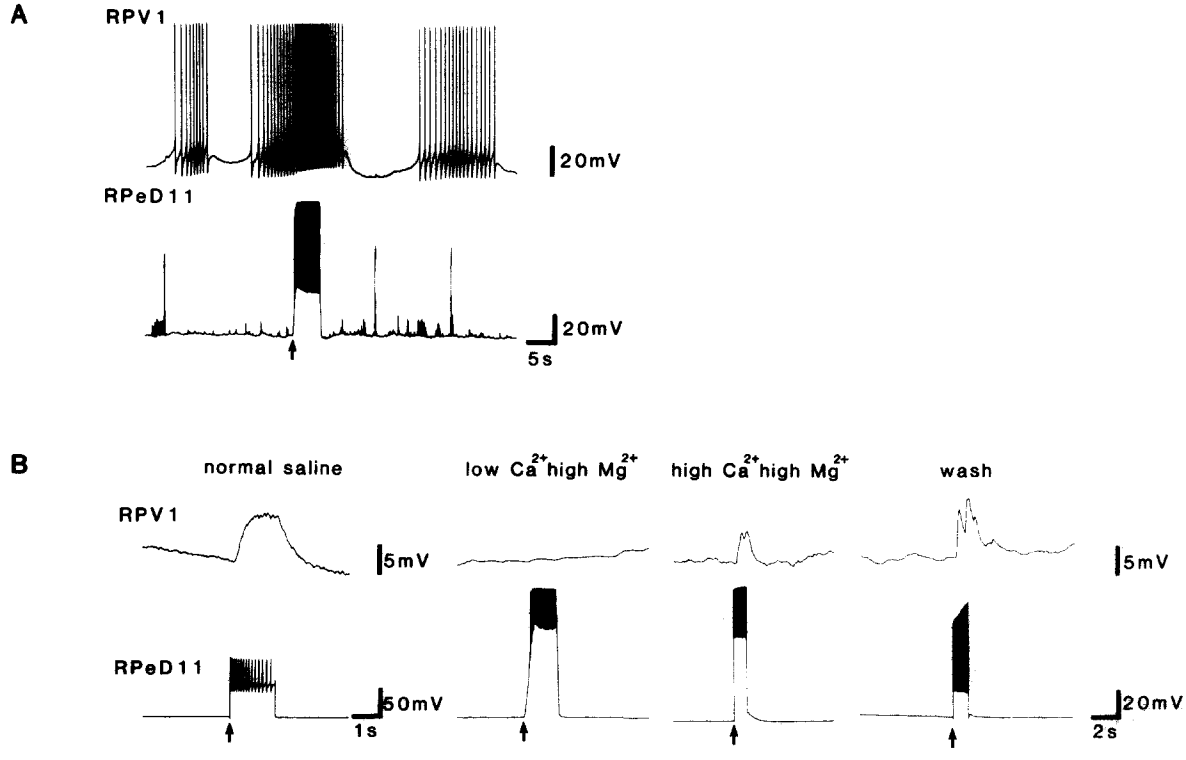


Fig. 8. Interneuron RPeD11 excites neuron RPV1. A: when neuron RPeD11 is stimulated (at arrow) it produces excitation and an increased frequency of firing in neuron RPV1. B: synaptic physiology of the RPeD11 to RPV1 synapse. The first panel shows that stimulation of neuron RPeD11 produces a summed EPSP in neuron RPV1. The second and third panels show how this connection was eliminated by low $Ca^{2+}$/high $Mg^{2+}$ saline but persisted in high $Ca^{2+}$/high $Mg^{2+}$ saline. Throughout the experiment documented in part B, neuron RPV1 was hyperpolarized in order to reveal distinct EPSPs.

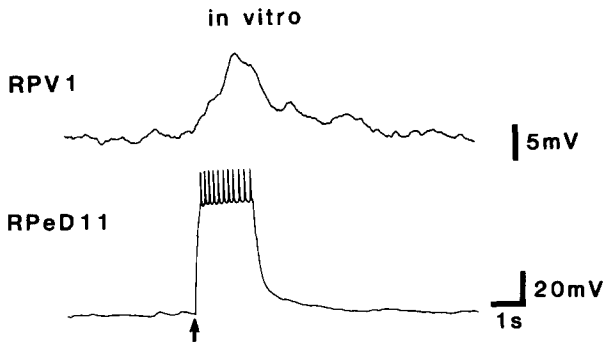


Fig. 9. The RPeD11 to RPV1 synapse in vitro. The recording is taken from a one day culture of two neurons which have established physical contact through newly sprouted neurites. Stimulation of neuron RPeD11 (at arrow) produced a summed EPSP in neuron RPV1.

an altered (multiphasic) form following perfusion of salines containing high levels of divalent cations (see the last two panels of Fig. 8B). The reason for this change is unknown, but high divalent salines are known to produce multiphasic PSPs in *Tritonia* cerebral interneurons [19].

Identified cell culture was employed to test if the connection between RPeD11 and RPV1 observed in the isolated brain could be re-established in vitro. Neurons RPV1 and RPeD11 were identified, isolated, and plated on poly-L-lysine coated dishes in CM. Under these conditions, the cells exhibited physical contact in the form of overlapping neurite outgrowth – suggesting the possibility of synaptic contact. Depolarization of neuron RPeD11 produced a summed excitatory postsynaptic potential (EPSP) in neuron RPV1 ($n = 5$) (Fig. 9). The EPSP was 5–10 mV in amplitude, which is comparable to the EPSP observed in situ. Electrical coupling, an inappropriate connection, was not observed between these two neurons in any of the five cell pairs tested.

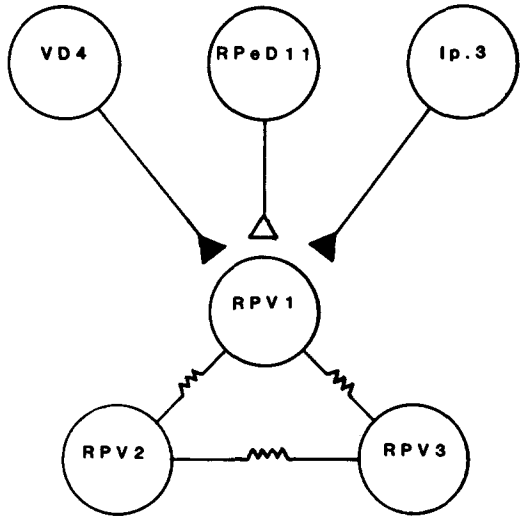


Fig. 10. Summary of the synaptic relationships between various interneurons and neurons RPV1–3. Depicted are the three interneurons, VD4, RPeD11, and Ip.3, with their different types of synaptic input onto the electrically coupled neurons RPV1–3. Symbols: excitatory chemical synapse (open triangle), inhibitory chemical synapse (closed triangle), and electrical synapse (—∿∿—).

## 4. Discussion

The morphology, electrophysiology, interconnections, and synaptic inputs of three neurons located in a largely neglected area of the *Lymnaea* CNS, i.e., the ventral surface, have been described. These cells are designated as RPV1–3 and they can be distinguished on the basis of both anatomy (size, color, location, morphology) and electrophysiology (firing pattern, action potential half-width, electrical coupling). These neurons receive synaptic inputs from several previously identified interneurons.

### *4.1. Bursting activity in neuron RPV1*

Bursting activity in neurons, especially molluscan neurons, has been studied extensively [1,2,27]. The nature of the bursting, i.e., whether it is endogenous or conditional upon synaptic input, has been one of the main areas of study in this field. Given such an interest, it is worth discussing neuron RPV1's bursting activity further. A brief description of neuron RPV1 was given by Winlow and Benjamin [55], who demonstrated that a burst of action potentials in neuron RPV1 could be correlated with an unidentified synaptic input appearing in another neuron known as visceral ventral one (VV1). The burst appeared ~ 500 ms after the occurrence of the synaptic input in VV1 – suggesting that the unidentified synaptic input drives the burst and that neuron RPV1 is a conditional burster. In the present study, cell culture was employed to investigate the activity of neuron RPV1 in the absence of synaptic input. Under the conditions of isolation, neuron RPV1 did not exhibit distinct bursting; however, when depolarizing current was injected into the cell it fired bursts of action potentials similar to that observed in situ (see Fig. 5B). In fact, an induced burst ended with a depolarizing afterpotential (compare Figs. 1A and 5B) – a characteristic of burst termination in neurons such as R15 of *Aplysia* [1]. Both the in vitro and in situ, the depolarizing afterpotential appears only at the end of a distinct burst, it does not appear at the end of a single action potential within the burst (see Fig. 3B). There are some examples of depolarizing afterpotentials appearing at the end of single spikes, such as in some *Tritonia* buccal neurons [12], but neuron RPV1 does not behave in this fashion. These findings, together with the data from

Winlow and Benjamin [55], strongly suggest that neuron RPV1 is a conditional and not an endogenous burster. However, the source of the conditional input is as yet unknown.

### 4.2. Synapse formation in vitro

The use of identified cell culture to study the properties of neurons RPV1–3 was taken one step further by re-establishing, in vitro, a specific synaptic connection – the RPeD11 to RPV1 synapse. When the cells were cultured together they formed an appropriate chemical excitatory synapse from neuron RPeD11 to neuron RPV1 (see Fig. 9). Previous synaptogenesis studies in *Lymnaea* have demonstrated that interneurons, such as neuron VD4, usually form synapses only with cells that they are monosynaptically connected to in vivo [45,46]. This fact, along with the data presented here, strengthens the hypothesis that interneuron RPeD11 is monosynaptically connected to neuron RPV1. This is the first demonstration that this particular *Lymnaea* interneuron is capable of appropriate synaptogenesis. Regarding monosynaptic connections in vivo, interneurons such as VD4 and RPeD11 usually elicit compound postsynaptic potentials (PSPs) in their follower cells, with no one-to-one ratio between presynaptic spikes and PSPs [19,42–44,47]. Consequently, definitive proof of a monosynaptic connection, such as a one-to-one/spike-to-PSP relationship in high $Ca^{2+}$/high $Mg^{2+}$ saline, is rarely attainable. The demonstration of in vitro synaptogenesis between two neurons provides support, albeit circumstantial, that a monosynaptic connection may exist in vivo [45,46,48].

Specific synapse formation is not unique to *Lymnaea*. Work on leech and the molluscs *Aplysia* and *Helisoma* has also demonstrated the ability of neurons to establish appropriate connections in vitro [14,33,34,46,48]. However, there are several instances, from both *Helisoma* and *Aplysia*, where neurons not connected in vivo will form synapses in vitro [23,39]. Thus, one must have prior evidence that the neurons in question *may* be monosynaptically connected in vivo, before making any conclusions from in vitro synapse formation. Evidence presented in the present study suggests that neurons RPeD11 and RPV1 are monosynaptically connected in vivo, and the occurrence of in vitro synapse formation between these neurons supports such a suggestion.

### 4.3. The location and morphology of neurons RPV1–3

The neural network that has been described encompasses an important new section in the ever expanding circuitry map of *Lymnaea's* CNS. These findings increase our knowledge of the ventral surface of *Lymnaea's* CNS. With the exception of the pedal and buccal ganglia [29,37], the ventral surface is not well characterized and there are very few examples of neuronal mapping of neurons on the ventral surface of *Lymnaea's* central ring ganglia. Neurons RPV1–3 receives input from interneurons VD4 and RPeD11. These interneurons are imbedded in a network of cells responsible for cardiorespiratory, locomotor, and defensive behavior [18,42,44,56]. This network, comprised of mainly motor neurons in the cerebral, pedal, and visceral ganglia, is coordinated and modulated by interneurons like RPeD11 and VD4 [42,44,56]. Thus neurons RPV1–3 are probably part of a network consisting of many identified neurons and neuronal clusters.

Because of the location of neurons RPV1–3, i.e., the ventral surface of the right parietal ganglion, an important issue to address is whether or not these cells are part of an identified neuronal cluster known as the light yellow cells (LYCs). The LYCs are a group of putative neurosecretory cells which are also located on the ventral surface of the right parietal ganglion [52]. However, it is unlikely that neurons RPV1–3 are members of the LYC cluster. This conclusion is based on the fact that the LYC cluster is more lateral and posterior compared to neurons RPV1–3, the LYCs have smaller soma diameters (50–80 $\mu$m) than neurons RPV1–3 [51], their firing patterns are dissimilar to neurons RPV1–3 [8,51], and they receive little or no synaptic input [51].

The morphology of neurons RPV1–3 exhibited some variability (Table 1). In neurons RPV2&3, a small number of variant axonal projections were present in some preparations. This is not surprising, variations in the morphology of identified neurons has been previously reported for both *Lymnaea* and *Aplysia* [5,22,29, 58]. It has been suggested that such variations reflect a form of developmental plasticity [58]; however, the functional consequence of this variability is unknown.

Determining the exact behavioral roles of neurons RPV1–3 is beyond the scope of the present study; however, some speculations regarding the function of these neurons can be made. For example, neurons RPV2&3 project axons through nerves of the right pedal ganglion. These nerves innervate foot and body wall musculature [56] implicating neurons RPV2&3 in locomotory or withdrawal behavior. Furthermore, interneuron RPeD11, which coordinates locomotion and withdrawal behavior [44], has excitatory effects on neuron RPV1 – the electrically coupled partner of neurons RPV2&3. Neurons RPV1–3 also send axons through the right internal parietal nerve (see Fig. 2), which innervates the pneumostome (breathing pore) of *Lymnaea* [41]. Such a projection may implicate neurons RPV1–3 in respiration; however, because neurons RPV1–3 are inhibited by respiratory pattern generator neurons VD4 and Ip3 (see Figs. 6&7), a role in

respiration seems unlikely, but this further implicates them in locomotion (a behavior incompatible with respiration in this animal).

## Acknowledgements

The authors thank Mr. G.C. Hauser for excellent technical support and Ms. N.M. Ewadinger for both assistance in the production of figures and comments on earlier drafts of the manuscript. This work was supported by grants from the Medical Research Council (MRC) of Canada (to A.G.M.B.) and the Alberta Lung Association (to N.I.S.). N.S. Magoski is a recipient of MRC, Alberta Heritage Foundation for Medical Research (AHFMR), and Network of Centres of Excellence studentships, N.I. Syed is a Parker B. Francis Scholar, AHFMR Scholar, and Alfred P. Sloan Fellow, and A.G.M. Bulloch is an AHFMR Scientist.

## References

[1] Adams, W.B. and Benson, J.A., The generation and modulation of endogenous rhythmicity in the *Aplysia* bursting pacemaker neurone R15, *Prog. Biophys. Mol. Biol.*, 46 (1985) 1–49.

[2] Alevizos, A., Skelton, M., Weiss, K.R. and Koester, J., A comparison of bursting neurons in *Aplysia*, *Biol. Bull.*, 180 (1991) 269–275.

[3] Audesirk, T. and Audesirk, G., Behavior of gastropod molluscs. In A.O.D. Willows (Ed.), *The mollusca, Vol. 8*, Academic, London, 1985, pp. 1–94.

[4] Austin, G., Yai, H. and Sato, M., Calcium ion effects on *Aplysia* membrane potentials. In C.A.G. Wiersma (Ed.), *Invertebrate nervous systems*, University of Chicago, IL, 1967, pp. 39–53.

[5] Benjamin, P.R., Interganglionic variation in cell body location of snail neurons does not affect synaptic connections or central axonal projections, *Nature*, 260 (1976) 338–340.

[6] Benjamin, P.R., Interneuronal network acting on snail neurosecretory neurons (yellow cells and yellow green cells of *Lymnaea*, *J. Exp. Biol.*, 113 (1984) 165–185.

[7] Benjamin, P.R., Elliott, C.J.H. and Ferguson, G.P., Neural network analysis in the snail brain. In A. Selverston (Ed.), *Model Networks and Behavior*, Plenum, New York, 1985, pp 87–108.

[8] Benjamin, P.R. and Swindale, N.V., Electrical properties of 'dark green' and 'yellow' neurosecretory cells in the snail *Lymnaea stagnalis*, *Nature*, 258 (1975) 622–623.

[9] Benjamin, P.R. and Winlow, W., The distribution of three wide-acting synaptic inputs to identified neurons in the isolated brain of *Lymnaea stagnalis* (L.), *Comp. Biochem. Physiol.*, 70 (1981) 293–307.

[10] Berry, M.S. and Pentreath, V.W., Criteria for distinguishing between monosynaptic and polysynaptic transmission, *Brain Res.*, 105 (1976) 1–20.

[11] Buckett, K.J., Peters, M. and Benjamin, P.R., Excitation and inhibition of the heart of the snail, *Lymnaea*, by non-FMRFamidergic motoneurons, *J. Neurophysiol.*, 63 (1990) 1436–1447.

[12] Bulloch, A.G.M. and Willows, A.O.D., Physiological basis of feeding in *Tritonia diomedea*. III. Role of depolarizing afterpotentials, *J. Neurobiol.*, 12 (1981) 515–532.

[13] Bulloch, A.G.M. and Syed, N.I., Reconstruction of neuronal networks in culture, *Trends Neurosci.*, 15 (1992) 422–427.

[14] Camardo, J., Proshansky, E. and Schacher, S., Identified *Aplysia* neurons form specific chemical synapses in culture, *J. Neurosci.*, 3 (1983) 2614–2620.

[15] Chen, C.F., von Baumgarten, R. and Takeda, R., Pacemaker properties of completely isolated neurons in *Aplysia californica*, *Nature New Biol.*, 233 (1971) 27–29.

[16] Elliott, C.J.H. and Benjamin, P.R., Interactions of pattern generating interneurons controlling feeding in *Lymnaea stagnalis*, *J. Neurophysiol.*, 54 (1985), 1396–2620.

[17] Elliott, C.J.H. and Benjamin, P.R., Esophageal mechanoreceptors in the feeding system of the pond snail, *Lymnaea stagnalis*, *J. Neurophysiol.*, 61 (1989), 727–736.

[18] Ferguson, G.P. and Benjamin, P.R., The whole-body withdrawal response of *Lymnaea stagnalis* I. identification of central motoneurones and muscles, *J. Exp. Biol.*, 158 (1991) 63–95.

[19] Getting, P.A., Mechanisms of pattern generation underlying swimming in *Tritonia*. I. Neuronal network formed by monosynaptic connections, *J. Neurophysiol.*, 46 (1981) 65–79.

[20] Getting, P.A., Neural control of behavior in gastropods. In A.O.D. Willows (Ed.), *The mollusca, Vol. 8*, Academic, London, 1985, pp. 269–334.

[21] Hawver, D.B. and Schacher, S., Selective fasciculation as a mechanism for the formation of specific chemical connections between *Aplysia* neurons *in vitro*, *J. Neurobiol.*, 24 (1993) 368–383.

[22] Haydon, P.G. and Winlow, W., Morphology of the giant dopamine-containing neuron, R.Pe.D.1, in *Lymnaea stagnalis* revealed by Lucifer Yellow CH, *J. Exp. Biol.*, 94, (1981) 149–157.

[23] Haydon, P.G., Formation of chemical synapses: neuronal strategies. In A.G.M. Bulloch (Ed), *The Cellular Basis of Neuronal Plasticity, Studies in Neurosciences #7*, Manchester University, Manchester, 1989, pp. 129–151.

[24] Jacklet, J.W. (Ed), *Neuronal and Cellular Oscillators*, Marcel Decker, New York, 1988.

[25] Kandel, E.R., *The Cellular Basis of Behavior*, Freeman, San Francisco, 1976.

[26] Kandel, E.R., *Behavioral Biology of Aplysia*, Freeman, San Francisco, 1979.

[27] Kater, S.B. and Kaneko, C.R.S., An endogenous bursting neuron in the gastropod mollusc, *Helisoma trivolvis* characterization of activity *in vivo*, *J. Comp. Physiol.*, 79 (1972) 114.

[28] Kristan Jr., W.B., Neuronal basis of behavior, *Curr. Opin. Neurobiol.*, 22 (1992) 781–787.

[29] Kyriakides, M., McCrohan, C.R., Slade, C.T., Syed, N.I. and Winlow, W., The morphology and electrophysiology of the neurones of the paired pedal ganglia of *Lymnaea stagnalis* (L.), *Comp. Biochem. Physiol.*, 93 (1989) 861–876.

[30] McCrohan, C.R. and Benjamin, P.R., Synaptic relationships of the cerebral giant cells with motoneurones in the feeding system of *Lymnaea stagnalis*, *J. Exp. Biol.*, 85 (1980) 169–186.

[31] Minium, E.W. and Clarke, R.B., *Elements of Statistical Reasoning*, Wiley, Toronto, 1982.

[32] Mpitsos, G.J. and Lukowiak, K., Learning in gastropod molluscs. In A.O.D. Willows (Ed.), *The mollusca, Vol. 8*, Academic, London, 1985, pp. 95–267.

[33] Rayport, S.G. and Schacher, S., Synaptic plasticity *in vitro*: cell culture of identified *Aplysia* neurons mediating short-term habituation and sensitization, *J. Neurosci.*, 6 (1986) 759–763.

[34] Ready, D.F. and Nicholls, J.G., Identified neurones isolated from leech CNS make selective connections in culture, *Nature*, 281 (1979) 67–69.

[35] Ridgway, R.L., Syed, N.I., Lukowiak, K. and Bulloch, A.G.M., Nerve growth factor (NGF) induces sprouting of specific neurons of the snail, *Lymnaea stagnalis*, *J. Neurobiol.*, 22 (1991) 377–390.

[36] Rose, R.M. and Benjamin, P.R., Interneuronal control of feeding in the pond snail *Lymnaea stagnalis* I. Initiation of feeding cycles by a single buccal interneurone, *J. Exp. Biol.*, 92 (1981) 187–201.

[37] Rose, R.M. and Benjamin, P.R., Interneuronal control of feeding in the pond snail *Lymnaea stagnalis* II. The interneuronal mechanism generating feeding cycles, *J. Exp. Biol.*, 92 (1981) 203–228.

[38] Schacher, S. and Proshansky, E., Neurite regeneration by *Aplysia* neurons in dissociated cell culture: modulation by *Aplysia* hemolymph and the presence of the initial axon segment, *J. Neurosci.*, 3 (1983) 2403–2413.

[39] Schacher, S., Rayport, S.G. and Ambron, R.T., Giant *Aplysia* neuron R2 reliably forms strong chemical synapses *in vitro*, *J. Neurosci.*, 5 (1985) 2851–2856.

[40] Selverston, A. (Ed.), *Model Networks and Behavior*, Plenum, New York, 1985.

[41] Slade, C.T., Mills, J. and Winlow, W., The neuronal organisation of the paired pedal ganglia of *Lymnaea stagnalis* (L.), *Comp. Biochem. Physiol.*, 69A (1981) 789–803.

[42] Syed, N.I. and Winlow, W., Morphology and electrophysiology of neurons innervating the ciliated locomotor epithelium in *Lymnaea stagnalis*, *Comp. Biochem. Physiol.*, 93, (1989) 633–644.

[43] Syed, N.I. and Winlow, W., Respiratory behavior in the pond snail *Lymnaea stagnalis* II. Neural elements of the central pattern generator (CPG), *J. Comp. Physiol.*, 169A (1991) 557–768.

[44] Syed, N.I. and Winlow, W., Coordination of locomotor and cardiorespiratory networks of *Lymnaea stagnalis* by a pair of identified interneurones, *J. Exp. Biol.*, 158 (1991) 37–62.

[45] Syed, N.I., Bulloch, A.G.M. and Lukowiak, K., In vitro reconstruction of the respiratory central pattern generator of the mollusk *Lymnaea*, *Science*, 250 (1990) 282–285.

[46] Syed, N.I., Lukowiak, K. and Bulloch, A.G.M., Specific *in vitro* synaptogenesis between identified *Lymnaea* and *Helisoma* neurons, *NeuroReport*, 3 (1992) 793–796.

[47] Syed, N.I., Harrison, D. and Winlow, W., Respiratory behavior in the pond snail *Lymnaea stagnalis* I. Behavioral analysis and the identification of motor neurons, *J. Comp. Physiol.*, 169 (1991) 541–555.

[48] Syed, N.I., Roger, I., Ridgway, R.L., Bauce, L.G., Lukowiak, K. and Bulloch, A.G.M., Identification, characterisation, and *in vitro* reconstruction of an interneuronal network of the snail *Helisoma trivolvis*, *J. Exp. Biol.*, 174 (1993) 19–44.

[49] ter Maat, A., Pieneman, A.W., van Duivenboden, Y.A. and Jansen, R.F., Identification of the pattern of penis innervation in the pond snail *Lymnaea stagnalis*, *Soc. Neurosci. Abstr.*, 17 (1991) 1402.

[50] van der Wilt, G.J., van der Roest, M. and Janse, C., Neuronal substrates of respiratory behavior and related functions in *Lymnaea stagnalis*. In H.H. Boer, W.P.M. Geraerts and E. Joosse (Eds.), *Neurobiology Molluscan Models*, North-Holland, Amsterdam, 1987, pp. 292–296.

[51] van Swigchem, H., On the endogenous bursting properties of 'light yellow neurosecretory cells in the freshwater snail' *Lymnaea stagnalis* (L.), *J. Exp. Biol.*, 80 (1979) 55–67.

[52] Wendelaar Bonga, S.E., Ultrastructure and histochemistry of neurosecretory cells and neurohaemal areas in the pond snail *Lymnaea stagnalis* (L.), *Z. Zellforsch.*, 108 (1970) 190–224.

[53] Wildering, W.C., Janse, C. and de Vlieger, T.A., The role of pacemaker properties and synaptic input in generation and modulation of spiking activity in a pair of electrically coupled peptidergic neurons, *Brain Res.*, 556 (1991) 324–328.

[54] Winlow, W., The plastic nature of action potentials. In A.G.M. Bulloch (Ed.), *The Cellular Basis of Neuronal Plasticity*, Manchester University Press, Manchester, 1989, pp. 3–27.

[55] Winlow, W. and Benjamin, P.R., Neuronal mapping of the brain of the pond snail *Lymnaea stagnalis* (L.). In J. Salanki (Ed.), *Neurobiology of Invertebrates, Gastropoda Brain*, Akademiai Kiado, Budapest, 1976, pp. 41–59.

[56] Winlow, W. and Haydon, P.G., A behavioural and neuronal analysis of the locomotory system *Lymnaea stagnalis*, *Comp. Biochem. Physiol.*, 83 (1986) 13–21.

[57] Winlow, W., Holden, A.V. and Haydon, P.G., Characterization of *Lymnaea* neurons by determination of action potential trajectories, *J. Exp. Biol.*, 99 (1982) 207–221.

[58] Winlow, W. and Kandel, E.R., The morphology of identified neurons in the abdominal ganglion of *Aplysia Californica*, *Brain Res.*, 112 (1976) 221–249.

[59] Wong, R.F., Barker, D.L., Kater, S.B. and Bodnar, D.A., Nerve growth-promoting factor produced in culture media conditioned by specific CNS tissues of the snail *Helisoma trivolvis*. *Brain Res.*, 292 (1984) 81–91.

[60] Wong, R.F., Hadley, R.D., Kater, S.B. and Hauser, G.C., Neurite outgrowth and cell cultures: the role of conditioning factor(s), *J. Neurosci.*, 1 (1981) 1008–1021.